ISSN 1070-3632, Russian Journal of General Chemistry, 2020, Vol. 90, No. 12, pp. 2410–2418. © Pleiades Publishing, Ltd., 2020.

Synthesis, In Vitro Antiproliferative Activity, and In Silico Studies of New Anilinoquinazoline Derivatives as Potential AntitumorAgents

M. K. Abdulwahab[a], R. Dzulkeflee[b], T. K. Han[c], R. A. Ruslan[d], K. H. Leong[c,*], C. H. Heh[c], and A. Ariffin[a,]**

[a] *Department of Chemistry, Faculty of Science, University of Malaya, Kuala Lumpur, 50603 Malaysia*
[b] *Department of Molecular Medicine, Faculty of Medicine, University of Malaya, Kuala Lumpur, 50603 Malaysia*
[c] *Department of Pharmaceutical Chemistry, Faculty of Pharmacy, University of Malaya, Kuala Lumpur, 50603 Malaysia*
[d] *Department of Biomedical Science, Faculty of Medicine, University of Malaya, Kuala Lumpur, 50603 Malaysia*
*e-mail: *azhar70@um.edu.my; **leongkh@um.edu.my*

Received September 21, 2020; revised October 15, 2020; accepted December 15, 2020

Abstract—A series of anilinoquinazoline derivatives with modification on the 2nd carbon of the aniline ring has been synthesized and characterized. The compounds have been tested for their in vitro antiproliferative activity against three NSCLC cell lines, including A549, H1650 and H1975. One of the products has demonstrated the highest IC_{50} value against A549 (17.60 ± 1.70 μM), surpassing the standard drug, gefitinib (34.32 ± 1.30 μM), another one has exhibited IC_{50} value against H1975 (9.75 ± 1.06 μM), surpassing gefitinib (31.12 ± 0.38 μM). The best performing derivatives in the antiproliferative assay have been selected for further in silico study for investigating their plausible binding mode in different EGFR kinases through molecular docking and molecular dynamics simulations.

Keywords: anilinoquinazoline, synthesis, antiproliferative activity, molecular docking, molecular dynamics

DOI: 10.1134/S1070363220120294

Quinazoline derivatives have demonstrated a broad spectrum of valuable biological activities, including antimicrobial [1], anti-inflammatory [2] and anticonvulsant [3]. Several derivatives of anilinoquinazoline, such as gefitinib and erlotinib, are widely used in treatment of non-small cell lung cancer (NSCLC) [4, 5]. Discovery of those anticancer agents has stimulated further attempts in derivatation of anilinoquinazoline scaffold and study of the products antitumor activity [6–9].

However, a limited attention has been payed to the derivatives with substituents on the 2nd carbon atom of the aniline ring of the anilinoquinazoline. Therefore, in this project, a series of anilinoquinazoline derivatives with an aromatic ring extended from an amide linker on the 2nd carbon of the aniline ring (Fig. 1) was synthesized and tested for antiproliferative activity against A549, H1650, and H1975 cell lines. Molecular docking and molecular dynamics simulations were involved for the insite in the mechanism of their cells proliferation inhibition.

RESULTS AND DISCUSSION

Eight new anilinoquinazoline derivatives were synthesized according to the synthetic pathway outlined in Scheme 1. The commercially available 2-amino-4-

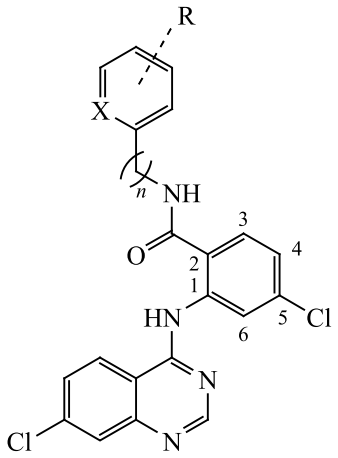

Fig. 1. General structure of the designed derivatives.

Scheme 1. Synthetic pathway to compounds **4a**–**4h**.

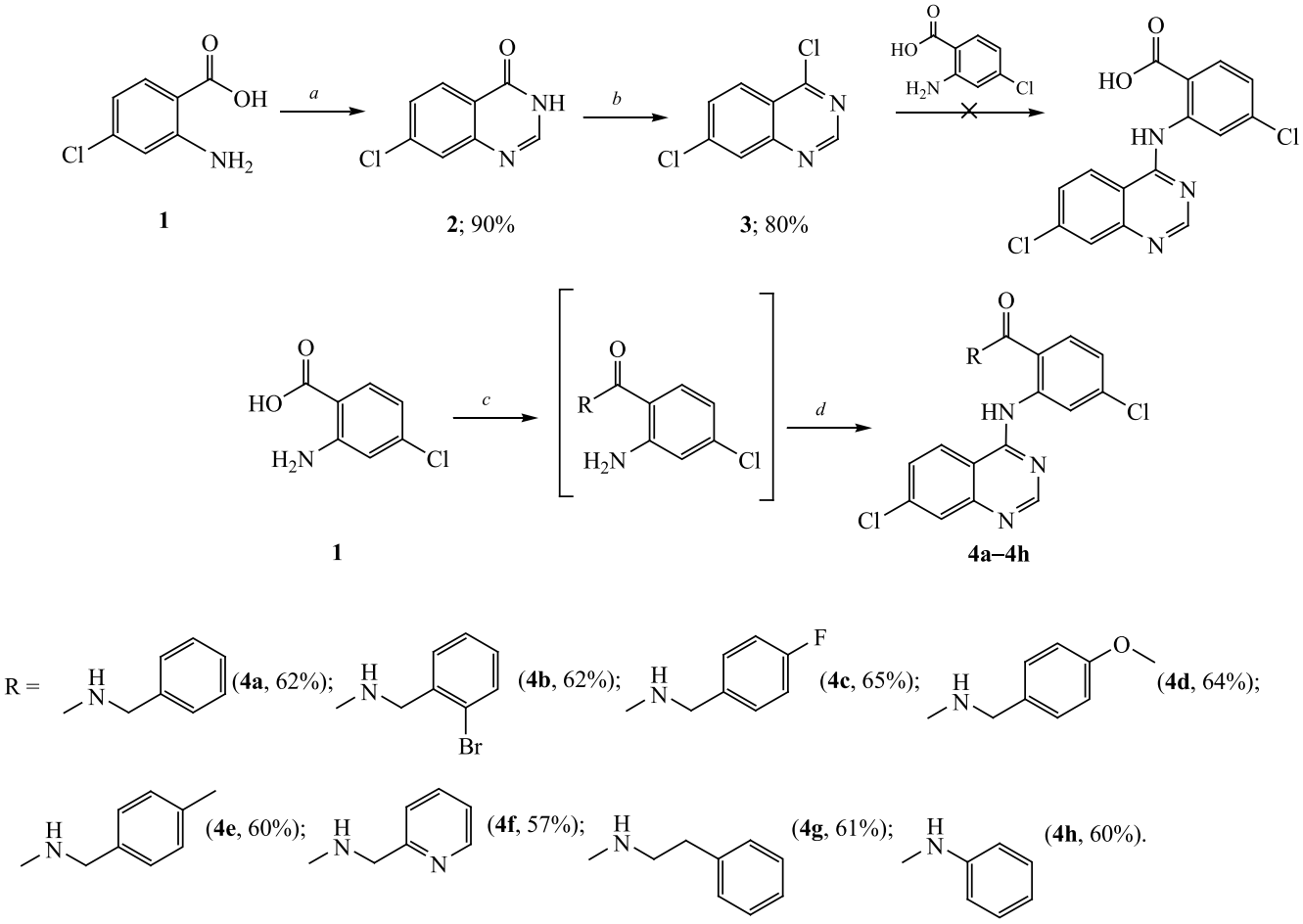

Reagents and conditions: (*a*) formamide, MW, 190°C, 0.5 h; (*b*) oxalyl chloride, DMF, $CHCl_3$, 60°C, overnight; (*c*) CDI, THF, different amines, room temperature, overnight; (*d*) 4,7-dichloroquinazoline, THF, room temperature, overnight.

chlorobenzoic acid (**1**) was reacted with formamide under MW irradiation to afford 7-chloroquinazolin-4(3*H*)-one (**2**). Initially the same process was carried out under conversion heating of **1** [10, 11]. The alternative MW irradiation [12] elevated the yield of **2** up to 90%.

Chlorination of 7-chloroquinazolin-4(3*H*)-one (**2**) using oxalyl chloride and DMF in chloroform produced 4,7-dichloroquinazoline (**3**) [13, 14], the following reaction of which with 2-amino-4-chlorobenzoic acid in THF targeted the 4-anilinoquinazoline scaffold. However, very low solubility of the precipitated product in common NMR solvents did not allow to characterize its structure. Instead, a series of aminobenzamide was prepared in situ from 2-amino-4-chlorobenzoic acid and different amines via CDI mediated coupling, before being reacted with 4,7-dichloroquinazoline (**3**) with formation of the target compounds **4a**–**4h** (Scheme 1).

Antiproliferative study. The in vitro antiproliferative activity of the synthesized compounds was measured against three NSCLC cell lines: A549, H1650, and H1975 (Table 1). Gefitinib was used as the positive control.

The products demonstrated different selectivity on the cell lines. In comparison with gefitinib, seven compounds (except **4f**) demonstrated better IC_{50} values on A549 cell line, and similarly, seven compounds (besides **4c**) performed better on H1975 cell line. However, none of the compounds performed better than gefitinib on H1650 cell line.

Compounds **4a**, **4g**, and **4h** were structurally different in term of the distance between the amido group and the phenyl ring. Specifically, there was one carbon atom separating the two groups in compound **4a,** two carbons in compound **4g**, and none in compound **4h**. On A549 cell line, compound **4a** (24.87 ± 1.74 μM) performed

Table 1. The IC_{50} values for compounds **4a**–**4h** and gefitinib

Compound	IC_{50} (Mean ± SD μM)		
	A549[a]	H1650[b]	H1975[c]
4a	24.87 ± 1.74	26.11 ± 1.62	23.83 ± 1.68
4b	27.14 ± 0.39	30.35 ± 0.89	28.28 ± 1.01
4c	26.18 ± 0.92	28.04 ± 1.75	32.23 ± 0.71
4d	23.78 ± 0.26	25.88 ± 1.26	23.49 ± 1.13
4e	17.60 ± 1.70	27.61 ± 0.49	20.46 ± 1.86
4f	44.54 ± 0.53	36.64 ± 0.20	21.11 ± 1.59
4g	31.06 ± 0.28	31.14 ± 1.31	9.75 ± 1.06
4h	33.64 ± 0.75	30.30 ± 1.63	29.66 ± 0.85
Gefitinib	34.32 ± 1.30	19.17 ± 1.90	31.12 ± 0.38

[a] A549 is NSCLC cell line with wild-type (WT) EGFR.
[b] H1650 is NSCLC cell line with exon 19 deletions mutated EGFR.
[c] H1975 is NSCLC cell line with L8585R+T790M (LRTM) mutated EGFR.

better than **4g** (31.06 ± 0.28 μM) and **4h** (33.64 ± 0.75 μM). On the other hand, on H1975 cell line, compound **4g** (9.75 ± 1.06 μM) exhibited better results than **4a** (23.83 ± 1.68 μM) and compound **4h** (29.66 ± 0.85 μM). Compound **4f** which contained pyridinyl ring instead of phenyl was determined to be of the lowest activity.

Molecular docking study. The molecular docking study was carried out for the most active products **4e** and **4g** interaction with EGFR kinase, which was chosen as the target protein [15, 16], and gefitinib and erlotinib were known as inhibitors of EGFR kinase [17].

Compound **4e** and compound **4g** were considered as ligands for docking in WT-EGFR and LRTM-EGFR, respectively (Table 2).

Compound **4e** bound to WT-EGFR could be in the same orientation in the crystal structure of erlotinib in EGFR kinase [4]. The incorporated aromatic ring on the 2nd position of the aniline ring of compound **4e** formed π–π interaction with PHE723. The aromatic ring also formed π-anion interaction with ASP855. π-Anion interaction with ASP855 had previously been observed in the docking of luteolin in EGFR kinase [18]. In LRTM-EGFR, compound **4g** also formed hydrogen bonding with MET793, and its aromatic ring was involved in π- π interactions with PHE723.

The 3D diagrams of both docking results indicated that LYS745 and ASP855 residues were in close proximity to the amide group linker of compounds **4e** and **4g.** Despite the ability of the amide group to become a hydrogen donor and acceptor, such interactions were not observed.

Molecular dynamics simulations. The molecular dynamics simulations were carried out for the compounds **4e** and **4g** in the respective kinases for detecting possibile H-bonds formation with the residues that could contribute to their in vitro antiproliferative activity.

Stability and fluctuation of the systems were evaluated by the root-mean-square deviation (RMSD) of the backbone residues over 50 ns, that were calculated by

Table 2. List of interactions for compound **4e** in WT-EGFR, and compound **4g** in LRTM-EGFR

Parameter	Compound **4e** in WT-EGFR	Gefitinib in WT-EGFR	Compound **4g** in LRTM-EGFR	Gefitinib in LRTM-EGFR
Hydrogen bonding	MET793[a]	MET793[a]	MET793[a]	[1]MET793
π–π interaction	PHE723[b]	–	PHE723[b]	–
π-Anion/Cation	ASP855	LYS745	–	–
Carbon hydrogen bond		GLN791, ASP855		ARG841
Van der Waals	GLU762, THR790, GLN971, LEU792, GLY796, THR854	LEU788, THR790, LEU792, GLY796, THR854, PHE856	GLU762, GLN791, LEU792, GLY796, THR854, ASP855, ARG858	GLY719, MET766, LEU788, LEU792, PRO794, GLY796, CYS797, THR854
Pi-Sigma	LEU718, LYS745, LEU844	LEU844	LEU718, LEU844	LEU718
Alkyl/Pi-Alkyl	VAL726, ALA743, MET766, LEU788	LEU718, PHE723, VAL726, ALA743, MET766	VAL726, ALA743, LYS745, MET766, LEU788,	VAL726, ALA743, LYS745, LEU844
Pi-Sulfur	–		MET790[c]	MET790[c]
Halogen		GLU762		GLU762

[a] The essential amino acid residues of the EGFR kinase for substrate binding at the active site [4].
[b] The targeted amino acid by aromatic ring incorporation.
[c] The mutated amino acid.

Table 3. The H-bond occupancy of compound **4e** and gefitinib in WT-EGFR and compound **4g** and gefitinib in LRTM-EGFR

Receptor	Ligand	Acceptor	Donor	Occupancy, %
WT-EGFR	**4e**	Compound **4e**-N[a]	MET793-NH[b]	88.24
		ASP_855-OD1[c]	Compound **4e**-N21[d]	5.04
		ASP_855-OD2[c]	Compound **4e**-N21[d]	3.68
	Gefitinib	Gefitinib-N[a]	MET793-NH[b]	91.80
LRTM-EGFR	**4g**	Compound **4g**-N[a]	MET793-NH[b]	95.88
		ASP855-OD2[c]	Compound **4g**-N21[d]	23.95
	Gefitinib	Gefitinib-N[a]	MET793-NH[b]	91.48

[a] N: the nitrogen atom of the quinazoline ring.
[b] NH: the hydrogen atom on the amino group of MET793.
[c] OD1 and OD2 are two different oxygen atoms of ASP855.
[d] N-21 is the nitrogen atom of the amide group of the compounds.

using their respective energy minimized structures as a reference. Ten amino acid residues of both terminals of each kinase were opted out from RMSD calculations due to their highly fluctuating nature that might interfere with the interpretation of the results [19]. According to RMSD of the complexes the backbones of those were stabilized after 30 ns of simulations.

Hydrogen bond occupancy (Table 3 and Supplementary Materials). Though both compounds **4e** and **4g** contained the amide group on their aniline ring, compound **4g** had a higher occupancy of the hydrogen bonding with ASP855 (23.95%), than **4e** (8.72%). The 3D interaction diagram of LRTM-EGFR/compound **4g** (Fig. 2a) supported the fact that presence of the bulky mutated arginine residue (ARG858) pushed ASP855 residue closer towards compound **4g**, allowing it to form stronger hydrogen bonding with ASP855, whereas in WT-EGFR, ASP855 residue had more space to be flexible due to smaller LEU858 (Fig. 2b).

EXPERIMENTAL

All chemicals were obtained from various commercial sources, and used as received. TLC was performed using MERCK 25 TLC plates 20×20 cm silica gel 60 F254 precoated aluminum plates. The spots were visualized under the UV light. Ethyl acetate:hexane system was used as an eluent. Flash column chromatography was performed using silica gel (0.063–0.2 mm) as the stationary phase. Melting points were measured in glass capillaries on a MELTEMP II, Laboratory Device. NMR spectra were measured on a JEOL ECX-400 MHz using

(a) (b)

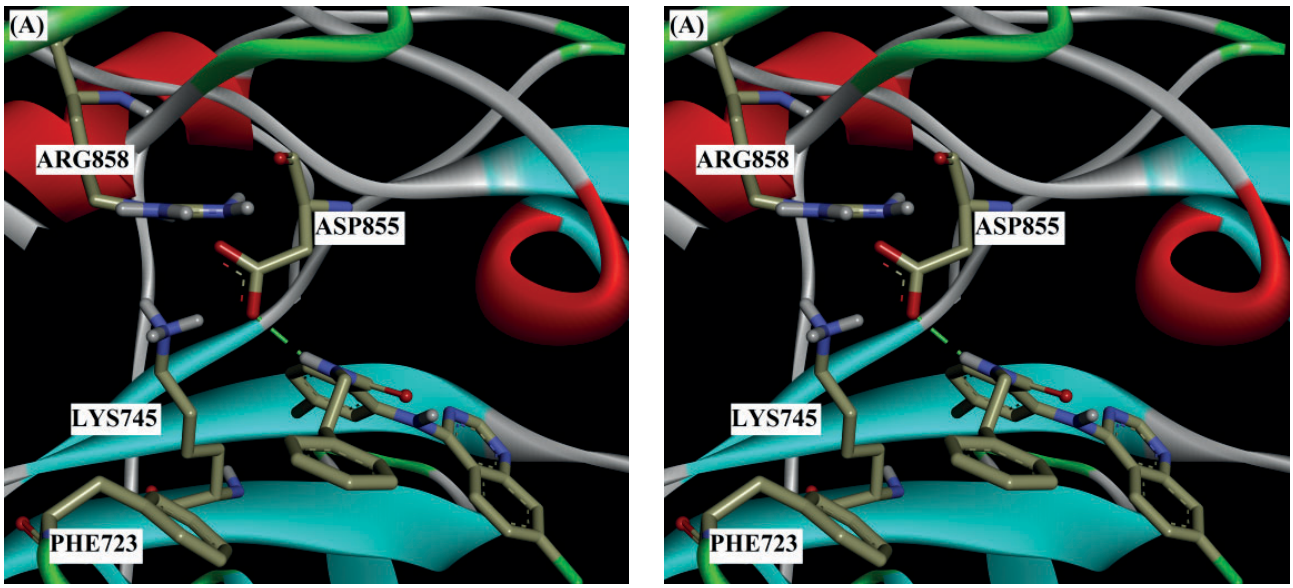

Fig. 2. 3D interaction diagrams of the lowest energy frame of (a) LTRM-EGFR/compound **4g**, and (b) WT-EGFR/compound **4e**.

DMSO-d_6 and $CDCl_3$ as the solvents. Mass spectra were measured on an Agilent 6550 iFunnel ESI-Q-TOF LC-MS.

Synthesis of 7-chloroquinazolin-4(3*H*)-one (2). 2-amino-4-chlorobenzoic acid (0.5 g, 2.91 mmol) was stirred in 7.5 mL of formamide. The mixture was heated in a microwave oven at 300 kWatt, 190°C, for 30 min. The clear brown reaction mixture was cooled to room temperature. Ice cold water was added to the reaction mixture to induce precipitation. The precipitate was filtered, and the crude product was further purified using column chromatography (EA: hexane, 7 : 3) to give compound **2** as white powder. Yield 90%, mp 256–258°C. ^{1}H NMR spectrum, δ, ppm: 7.49 d. d (1H, J = 8.71 Hz, J = 2.29 Hz, CH), 7.66 d (1H, J = 2.29 Hz, CH), 8.05 d (1H, J = 8.71 Hz, CH), 8.09 s (1H, CH), 12.35 s (1H, NH). ^{13}C NMR spectrum, δ_C, ppm: 122.0, 126.9, 127.5, 128.5, 139.4, 147.4, 150.4, 160.7.

Synthesis of 4,7-dichloroquinazoline (3). Compound **2** (5 g, 27.69 mmol) and DMF (1 mL, 20% w/w) were added to 150 mL of chloroform. The reaction mixture was cooled in an ice-bath. Oxalyl chloride (4.8 mL, 55.38 mmol) was added dropwise to the reaction mixture which was left to warm up to room temperature upon stirring for 2 h. Then the reaction mixture was heated to 60ºC and stirred overnight, upon completion of the process it was cooled in ice-bath. Then, 4.95 g of sodium hydrogen carbonate in 50 mL of cold water were added drop-wise to the reaction mixture. The mixture was separated, and the organic layer was dried using sodium sulphate and concentrated under vacuum. The crude product was purified by column chromatography (ethyl acetate: hexane, 1 : 1) to give the product **3** as white solid. Yield 80%, mp 140–142°C. ^{1}H NMR spectrum, δ, ppm: 7.67 d. d (1H, J = 8.70 Hz, J = 1.84 Hz, CH), 8.07 d (1H, J = 1.84 Hz, CH), 8.21 d (1H, J = 8.70Hz, CH), 9.04 s (1H, CH). ^{13}C NMR spectrum, δ_C, ppm: 122.6, 127.4, 128.0, 130.4, 141.6, 151.7, 154.8, 162.5.

Synthesis of compounds 4a–4g. Solution of amino-4-chlorobenzoic acid (0.30 g, 1.75 mmol) in 10 mL of THF was mixed with CDI (0.34 g, 2.10 mmol), and the mixture was stirred for 1 h, after which the desired amine was added to the mixture, and it was stirred overnight. Upon completion of the reaction (TLC), the mixture was filtered through silica, and the eluate was concentrated on a rotary evaporator. The crude intermediate and compound **3** (0.35 g, 1.75 mmol) were dissolved in 10 mL of THF at room temperature and stirred overnight. The resulting precipitate was filtered off. The crude product was stirred in isopropanol for 1 h and filtered to give the corresponding pure product.

***N*-benzyl-4-chloro-2-[(7-chloroquinazolin-4-yl)-amino]benzamide (4a).** Phenylmethanamine (0.16 mL, 1.50 mmol) was used as the reactant. Yellowish powder, yield 62%, mp 208–210°C. ^{1}H NMR spectrum, δ, ppm: 4.40 d (2H, J = 5.88 Hz, CH_2), 7.15 m (5H, C_6H_5), 7.44 d (1H, J = 8.55 Hz, CH), 7.89 d (2H, J = 8.55 Hz, CH), 7.98 s (1H, CH), 8.37 d (1H, J = 8.55 Hz, CH), 8.43 s (1H, CH), 8.84 s (1H, CH), 9.43 t (1H, J = 5.88 Hz, NH), 12.82 s (1H, NH). ^{13}C NMR spectrum, δ_C, ppm: 43.2, 113.5, 122.3, 124.8, 125.2, 125.8, 126.0, 127.4, 127.8, 128.8, 129.7, 130.0, 136.5, 138.8, 139.2, 140.6, 143.5, 153.4, 159.1, 167.4. MS: *m/z:* 423.0769 $[M + H]^+$.

***N*-(2-Bromobenzyl)-4-chloro-2-[(7-chloro-quinazolin-4-yl)amino]benzamide (4b).** (2-Bromo-phenyl)methanamine (0.19 mL, 1.50 mmol) was used as the reactant. Yellowish powder, yield 62%, mp 206–208°C. ^{1}H NMR spectrum, δ, ppm: 4.44 d (2H, J = 2.28 Hz, CH_2), 7.14 d. d (1H, J = 7.90 Hz, J = 7.34 Hz, CH), 7.23 d. d (1H, J = 7.90 Hz, J = 7.34 Hz, CH), 7.29 d (1H, J = 7.34 Hz, CH), 7.45 d (1H, J = 8.47 Hz, CH), 7.53 d (1H, J = 7.90 Hz, CH), 7.86 d (1H, J = 8.47 Hz, CH), 7.94 d (1H, J = 8.47 Hz, CH), 7.96 s (1H, CH), 8.33 d (1H, J = 8.47 Hz, CH), 8.49 s (1H, CH), 8.87 s (1H, CH), 9.44 s (1H, NH), 12.79 s (1H, NH). ^{13}C NMR spectrum, δ_C, ppm: 43.8, 113.7, 122.9, 124.4, 124.6, 125.6, 125.9, 128.2, 129.4, 129.6, 131.0, 132.9, 136.7, 137.5, 139.2, 140.4, 144.2, 153.7, 158.9, 167.7. MS, *m/z:* 500.9893 $[M + H]^+$.

4-Chloro-2-[(7-chloroquinazolin-4-yl)amino]-*N*-(4-fluorobenzyl)benzamide (4c). (4-Fluorophenyl)-methanamine (0.17 mL, 1.50 mmol) was used as the reactant. White powder, yield 65%, mp 228–230°C. ^{1}H NMR spectrum, δ, ppm: 4.36 d (2H, J = 5.64 Hz, CH_2), 6.97 m (2H, CH), 7.23 m (2H, CH), 7.44 d (1H, J = 8.47 Hz, CH), 7.86 d (1H, J = 8.47 Hz, CH), 7.91 d (1H, J = 8.47 Hz, CH), 7.98 s (1H, CH), 8.38 m (2H, CH), 8.86 s (1H, CH), 9.43 s (1H, NH), 12.78 s (1H, NH). ^{13}C NMR spectrum, δ, ppm: 42.5, 113.3, 115.3, 121.6, 125.0, 126.8, 129.7, 129.9, 131.0, 135.5, 136.4, 138.4, 140.8, 142.7, 153.2, 159.3, 160.5, 162.9, 167.2. MS: *m/z:* 441.0680 $[M + H]^+$.

4-Chloro-2-[(7-chloroquinazolin-4-yl)amino]-*N*-(4-methoxybenzyl)benzamide (4d). (4-Methoxyphenyl)-methanamine (0.20 mL, 1.50 mmol) was used as the reactant. White powder, yield 64%, mp 226–228°C. ^{1}H

NMR spectrum, δ, ppm: 3.77 s (3H, OCH_3), 4.32 d (2H, J = 5.64 Hz, CH_2), 6.70 d (2H, J = 7.90 Hz, CH), 7.11 d (2H, J = 7.90 Hz, CH), 7.43 d (1H, J = 8.47 Hz, CH), 7.85 d (1H, J = 8.47 Hz, CH), 7.89 d (1H, J = 8.47 Hz, CH), 7.97 s (1H, CH), 8.35 d (1H, J = 8.47 Hz, CH), 8.39 s (1H, CH), 8.86 s (1H, CH), 9.34 s (1H, NH), 12.81 s (1H, NH). ^{13}C NMR spectrum, δ, ppm: 42.6, 55.5, 113.5, 114.1, 122.3, 124.5, 125.5, 125.8, 126.0, 129.2, 129.6, 130.9, 131.0, 131.2, 136.4, 138.8, 140.5, 153.5, 158.7, 159.1, 167.2. MS: *m/z:* 453.0861 $[M + H]^+$.

4-Chloro-2-[(7-chloroquinazolin-4-yl)amino]-*N*-(4-methylbenzyl)benzamide (4e). *p*-Tolylmethanamine (0.20 mL, 1.50 mmol) was used as the reactant. White powder, yield 60%, mp 226–228°C. ^{1}H NMR spectrum, δ, ppm: 2.19 s (3H, CH_3), 4.33 d (2H, J = 5.64 Hz, CH_2), 6.95 d (2H, J = 7.90 Hz, CH), 7.06 d (2H, J = 7.90 Hz, CH), 7.44 d. d (1H, J = 8.47 Hz, 2.26 Hz, CH), 7.85 d (1H, J = 8.47 Hz, CH), 7.89 d. d (1H, J = 9.03 Hz, 2.26 Hz, CH), 7.96 d (1H, J = 2.26 Hz, CH), 8.34 d (1H, J = 9.03 Hz, CH), 8.40 s (1H, CH), 8.85 s (1H, CH), 9.37 t (1H, J = 5.64 Hz, NH), 12.78 s (1H, NH). ^{13}C NMR spectrum, δ, ppm: 21.2, 42.9, 113.5, 122.2, 124.7, 125. 6, 125.9, 126.1, 127.8, 129.3, 129.6, 130.9, 136.2, 136.4, 136.5, 138.6, 140.5, 143.4, 153.4, 159.1, 167.2. MS: *m/z:* 437.0919 $[M + H]^+$.

4-Chloro-2-[(7-chloroquinazolin-4-yl)amino]-*N*-(pyridin-2-ylmethyl)benzamide (4f). Pyridin-2-ylmethanamine (0.15 mL, 1.50 mmol) was used as the reactant. White powder, yield 57%, mp 214–216°C. ^{1}H NMR spectrum, δ, ppm: 4.40 d (2H, J = 5.08 Hz, CH), 7.48 d. d (1H, J = 8.47 Hz, 1.70 Hz, CH), 7.65 d. d (1H, J = 5.64 Hz, 6.78 Hz, CH), 7.74 d (1H, J = 7.90 Hz, CH), 7.86 d. d (1H, J = 9.03 Hz, 1.69 Hz, CH), 7.97 (1H, d, J = 8.47 Hz, CH), 7.99 s (1H, CH), 8.18 d. d (1H, J = 6.78 Hz, 7.90 Hz, CH), 8.40 s (1H, CH), 8.42 d (1H, J = 9.03 Hz, CH), 8.65 d (1H, J = 5.64 Hz, CH), 8.87 s (1H, CH), 9.66 t (1H, J = 5.08 Hz, NH). ^{13}C NMR spectrum, δ, ppm: 42.2, 113.3, 121.5, 125.1, 125.4 (CH, C-23), 125.8, 126.4, 126.6, 129.6, 131.3, 136.6, 138.3, 140.8, 142.8, 143.6, 144.7, 153.1, 155.1, 159.5, 167.8. MS: *m/z:* 424.0718 $[M + H]^+$.

4-Chloro-2-[(7-chloroquinazolin-4-yl)amino]-*N*-phenethylbenzamide (4g). 2-Phenylethanamine (0.19 mL, 1.50 mmol) was used as the reactant. Yellowish powder, yield 61%, mp 216–218°C. ^{1}H NMR spectrum, δ, ppm: 2.78 t (2H, J = 7.34 Hz, CH), 3.40 m (2H, CH), 7.07 m (1H, CH), 7.19 m (4H, CH), 7.38 d. d (1H, J = 8.47 Hz, J = 1.70 Hz, CH), 7.78 d (1H, J = 8.47 Hz, CH), 7.91 d. d (1H, J = 8.47 Hz, J = 1.70 Hz, CH), 7.96 s (1H, CH), 8.26 d (1H, J = 8.47 Hz, CH), 8.64 s (1H, CH), 8.90 s (1H, CH), 9.03 t (1H, J = 5.64 Hz, NH), 12.88 s (1H, NH). ^{13}C NMR spectrum, δ, ppm: 35.2, 41.3, 114.0, 123.3, 123.5, 125.0, 125.6, 126.7, 127.3, 128.8, 129.2, 129.6, 130.7, 136.6, 139.4, 139.7, 140.3, 154.0, 158.6, 167.7. MS: *m/z:* 437.0911 $[M + H]^+$.

4-Chloro-2-[(7-chloroquinazolin-4-yl)amino]-*N*-phenylbenzamide (4h). Aniline (0.14 mL, 1.50 mmol) was used as the reactant. Yellowish powder, yield 60%, mp 216–218°C. ^{1}H NMR spectrum, δ, ppm: 7.03 t (1H, J = 7.34 Hz, CH), 7.25 d. d (2H, J = 7.90, 7.34 Hz, CH), 7.53 d (1H, J = 12.47 Hz, CH), 7.59 d (2H, J = 7.90 Hz, CH), 7.89 m (1H, CH), 7.91 m (1H, CH), 7.98 s (1H, CH), 8.12 s (1H, CH), 8.60 d (1H, J = 8.47 Hz, CH), 8.85 s (1H, CH), 10.66 s (1H, NH), 12.28 s (1H, NH). ^{13}C NMR spectrum, δ, ppm: 113.2, 121.1, 121.4, 124.7, 125.4, 126.3, 126.7, 128.7, 129.2, 129.7, 131.5, 136.2, 137.7, 139.1, 140.9, 142.4, 152.9, 159.7, 165.6. MS: *m/z:* 409.0591 $[M + H]^+$.

In vitro antiproliferative study. The in vitro antiproliferation activity of the synthesized derivatives was tested using the MTT assay. Gefitinib was used as the positive control. Three NSCLC cell lines, namely A549, H1650, and H1975 which were obtained from AddexBio Ltd. USA. DMEM was used as the media for A549 cell line, while RPMI 1640 was used as the media for H1650 and H1975 cell lines. The cells were cultured in a cell incubator at 37°C, where the humidified atmosphere of 5% CO_2 was maintained. The cells were plated into 96-wells microplate at a density of 10^4 cells per well after which the cells were incubated over a period of 24 h. The treatment of the test compounds onto the cells was executed using 100 μL of nine working concentrations (3.91–100 μM). The working solutions were prepared in 0.5% v/v DMSO in respective media. For negative control, the cells were treated with 100 μL of 0.5% v/v DMSO in media. The cells were incubated for another 72 h. Next, 20 μL of MTT reagent (5 mg/mL) were added to each well. After the MTT treatment, the cells were incubated for another 3 h. Then, the supernatant was removed carefully, after which 100 μL of DMSO was added to dissolve the MTT formazan crystals. The absorbance of the formazan product was read on a microplate reader at 570 nm, with 620 nm as the background wavelength (Infinite 200, Tecan, Männedorf, Switzerland). The percentage of the viable cells in each well was calculated from the absorbance of the respective well over that of the negative

control well. The IC_{50} values of the test compounds were determined from dose-response curves using Prism 8.0.2, software for Windows (GraphPad Software Inc., La Jolla, CA, USA). The results were expressed as mean ±standard deviation of triplicates [20].

Molecular docking. A workstation with four Intel Core 2 Duo E6850 3.00 GHz microprocessors, 8 GigaBytes of Random-Access Memory (RAM) and an Ubuntu 18.04 Linux operating system was used. Blind docking was performed on WT-EGFR and LRTM-EGFR using AutoDock Vina software [21]. The models for the kinases were obtained from the Protein Data Bank (PDB ID: 1M17 and 5EDR, respectively) [4, 22].

The present ligands and water molecules were removed from the kinases models using Biovia Discovery Studio Visualiser 4.5 software [23]. Then, AutoDockTools 1.5.6 software was used to add all hydrogen atoms, merging nonpolar hydrogen atoms, checking and repairing missing atoms, adding Gasteiger charges, assigning AD4 atom types to the protein structure, and finally saving the protein structure in .pdbqt format for further docking [24, 25]. A grid box of the kinase structure was then set using AutoDockTools 1.5.6 software with a grid spacing of 1.0 Å, dimensions of 126×126×126 points along the x, y and z axes, and centered on the kinase and covered the whole kinase for blind docking [26].

The structure of the ligands to be run in the molecular docking were constructed using ChemBio 3D Ultra 12.0, and their energy were minimized using MM2 energy minimization calculation [27]. Then, AutoDockTools 1.5.6 software was used to add flexibility to flexible bonds on the ligands and save the ligands in .pdbqt format as input files for molecular docking [24].

Molecular dynamics simulations. The MD simulations were carried out using GROMACS 2019 [28]. GROMACS "pdb2gmx" module with AMBER force field ff14SB [29] were used to prepare the receptor files for the simulations. Antechamber Python Parser Interface (ACPYPE) [30] software was used to prepare the ligand files, after which Generalized AMBER Force Field (GAFF) [31, 32] and AM1-BCC charge models were applied to the files. The receptor-ligand complex was suspended at the center of a TIP3P water box [33], where the edge of box was set to be at least 10 Å away from the complex. Explicit solvent model was used to solvate the system, after which the system was neutralized by adding counter ions prior to the energy minimization stage. The energy of the solvated system was minimized using the steepest descent algorithm, and followed by the conjugated gradient algorithm. After the energy minimization, equilibrium simulation was carried out with constant temperature and pressure at 300 K and 1 atm, respectively. All MD simulations during the production stage was carried out for 50 ns, while a trajectory was captured for every 20 ps. For RMSD calculation, the analysis of the collected trajectories was carried out using the GROMACS 'rms' module. For the hydrogen bond occupancy calculations, the trajectories collected from GROMACS MD simulation were converted into AMBER netcdf format (.nc) with cpptraj [34] module in AmberTools. The converted trajectories were then used for hydrogen bond occupancy analysis with cpptraj's hbond module.

CONCLUSIONS

Eight new anilinoquinazoline with an aromatic ring at the 2nd carbon of the aniline ring with amide group linker have been synthesized and tested for their in vitro antiproliferative activity against A549, H1650 and H1975 cell lines. The results have indicated that seven derivatives have demonstrated performance higher than that of gefitinib in A549 and H1975 cell lines, while none of the derivatives have performed better than the standard drug in H1650 cell line. Compound **4e** has demonstrated the best antiproliferative activity in A549 cell line (17.60 ± 1.70 μM), while compound **4g** has demonstrated the highest antiproliferative activity in H1975 cell line (9.75 ± 1.06 μM). The molecular docking study against EGFR kinases has proposed that both compounds have maintained the hydrogen bonding interaction with MET793 as observed in anilinoquinazoline derivatives, while forming the additional π–π stacking interaction with PHE723. Further in silico study by the molecular dynamics simulations has indicated that in WT-EGFR, compound **4e** could have interacted with ASP855 through the hydrogen bonding. In LRTM-EGFR, compound **4g** also could have form hydrogen bonding with ASP855. This study demonstrates that the incorporation of both amide group and phenyl ring on the 2nd carbon of the aniline ring increases the potency of the anilinoquinazoline derivatives against certain NCSLC cells. In conclusion, compound **4e** and compound **4g** can be considered as the potential leads for further development of antitumor agents.

FUNDING

This work was financially supported by the Ministry of Higher Education Malaysia, Fundamental Research Grant (FRGS/1/2019/SKK09/UM/02/1) and the University of Malaya Research Programme (RP035-17AFR).

CONFLICT OF INTEREST

The authors declare no conflict of interest in this work.

SUPPLEMENTARY INFORMATION

The online version contains supplementary material available at https://doi.org/10.1134/S1070363220120294.

REFERENCES

1. Raghavendra, N.M., Thampi, P., Gurubasavarajaswamy, P.M., and Sriram, D., *Chem. Pharm. Bull.,* 2007, vol. 55, p. 1615. https://doi.org/10.1248/cpb.55.1615
2. Manivannan, E. and Chaturvedi, S.C., *Bioorg. Med. Chem.,* 2011, vol. 19, p. 4520. https://doi.org/10.1016/j.bmc.2011.06.019
3. Georgey, H., Abdel-Gawad, N., and Abbas, S., *Molecules,* 2008, vol. 13, p. 2557. https://doi.org/10.3390/molecules13102557
4. Stamos, J., Sliwkowski, M.X., and Eigenbrot, C., *J. Biol. Chem.,* 2002, vol. 277, p. 46265. https://doi.org/10.1074/jbc.M207135200
5. Yun, C.H., Boggon, T.J., Li, Y., Woo, M.S., Greulich, H., Meyerson, M., and Eck, M.J., *Cancer Cell,* 2007, vol. 11, p. 217. https://doi.org/10.1016/j.ccr.2006.12.017
6. Yang, Z., Gu, J.-M., Ma, Q.-Y., Xue, N., Shi, X.-W., Wang, L., Zhang, K., Wang, Y.-B., Cao, D.-Y., Guo, R., and Xing, R.-J., *Future Med. Chem.,* 2019, vol. 11, p. 2821. https://doi.org/10.4155/fmc-2019-0220
7. Cheng, W., Wang, S., Yang, Z., Tian, X., and Hu, Y., *Drug Des. Devel. Ther.,* 2019, vol. 13, p. 3079. https://doi.org/10.2147/DDDT.S209481
8. Wei, H., Duan, Y., Gou, W., Cui, J., Ning, H., Li, D., Qin, Y., Liu, Q., and Li, Y., *Eur. J. Med. Chem.,* 2019, vol. 181, p. 111552. https://doi.org/10.1016/j.ejmech.2019.07.055
9. Hassan, H.M.A., Denetiu, I., Khan, S.A., Rehan, M., Sakkaf, K., and Gauthaman, K., *Med. Chem. Res.,* 2019, vol. 28, p. 1766. https://doi.org/10.1007/s00044-019-02413-6
10. Baumann, M. and Baxendale, I.R., *Beilstein J. Org. Chem.,* 2013, vol. 9, p. 2265. https://doi.org/10.3762/bjoc.9.265
11. Davoodnia, A., *Asian J. Chem.,* 2010, vol. 22, p. 1591.
12. Ouahrouch, A., Taourirte, M., Engels, J.W., Benjelloun, S., and Lazrek, H.B., *Molecules.,* 2014, vol. 19, p. 3638. https://doi.org/10.3390/molecules19033638
13. Shen, C., Wang, L., Wen, M., Shen, H., Jin, J., and Zhang, P., *Ind. Eng. Chem. Res.,* 2016, vol. 55, p. 3177. https://doi.org/10.1021/acs.iecr.5b04452
14. Min, J., Guo, K., Suryadevara, P.K., Zhu, F., Holbrook, G., Chen, Y., Feau, C., Young, B.M., Lemoff, A., Connelly, M.C., Kastan, M.B., and Guy, R.K., *J. Med. Chem.,* 2016, vol. 59, p. 559. https://doi.org/10.1021/acs.jmedchem.5b01092
15. Nicholson, R.I., Gee, J.M., and Harper, M.E., *Eur. J. Cancer,* 2001, vol. 37, p. S9-15. https://doi.org/10.1016/s0959-8049(01)00231-3
16. Harari, P.M., *Endocr. Relat. Cancer,* 2004, vol. 11, p. 689. https://doi.org/10.1677/erc.1.00600
17. Blackledge, G. and Averbuch, S., *Br. J. Cancer,* 2004, vol. 90, p. 566. https://doi.org/10.1038/sj.bjc.6601550
18. Ambrose, G.O., Afees, O.J., Nwamaka, N.C., Simon, N., Oluwaseun, A.A., Soyinka, T., Oluwaseun, A.S., and Bankole, S., *Bioinformation,* 2018, vol. 14, p. 241. https://doi.org/10.6026/97320630014241
19. Tiwari, G. and Mohanty, D., *PLoS One,* 2013, vol. 8, p. e71340. https://doi.org/10.1371/journal.pone.0071340
20. Nazarbahjat, N., Ariffin, A., Abdullah, Z., Abdulla, M.A., Shia, J.K.S., and Leong, K.H., *Med. Chem. Res.,* 2016, vol. 25, p. 2015. https://doi.org/10.1007/s00044-016-1660-5
21. Trott, O. and Olson, A.J., *J. Comput. Chem.,* 2010, vol. 31, p. 455. https://doi.org/10.1002/jcc.21334
22. Hanan, E.J., Baumgardner, M., Bryan, M.C., Chen, Y., Eigenbrot, C., Fan, P., Gu, X.-H., La, H., Malek, S., Purkey, H.E., Schaefer, G., Schmidt, S., Sideris, S., Yen, I., Yu, C., and Heffron, T.P., *Bioorg. Med. Chem. Lett.,* 2016, vol. 26, p. 534. https://doi.org/10.1016/j.bmcl.2015.11.078
23. BIOVIA, D.S., *Discovery Studio Visualizer*. 2016, Dassault Systèmes, San Diego.
24. Heh, C.H., Othman, R., Buckle, M.J.C., Sharifuddin, Y., Yusof, R., and Rahman, N.A., *Chem. Biol. Drug Des.,* 2013, vol. 82, p. 1. https://doi.org/10.1111/cbdd.12122
25. Morris, G.M., Huey, R., Lindstrom, W., Sanner, M.F., Belew, R.K., Goodsell, D.S., and Olson, A.J., *J. Comput.*

Chem., 2009, vol. 30, p. 2785. https://doi.org/10.1002/jcc.21256
26. Lim, S.K., Othman, R., Yusof, R., and Heh, C.H., *Curr. Comput. Aided Drug. Des.,* 2017, vol. 13, p. 160. https://doi.org/10.2174/1573409912666161130122622
27. Cousins, K.R., *J. Am. Chem. Soc.,* 2011, vol. 133, p. 8388. https://doi.org/10.1021/ja204075s
28. Abraham, M.J., Murtola, T., Schulz, R., Páll, S., Smith, J.C., Hess, B., and Lindahl, E., *SoftwareX,* 2015, vol. 1, p. 19. https://doi.org/10.1016/j.softx.2015.06.001
29. Maier, J.A., Martinez, C., Kasavajhala, K., Wickstrom, L., Hauser, K.E., and Simmerling, C., *J. Chem. Theory Comput.,* 2015, vol. 11, p. 3696. https://doi.org/10.1021/acs.jctc.5b00255
30. Sousa da Silva, A.W. and Vranken, W.F., *BMC Res. Notes,* 2012, vol. 5, p. 367. https://doi.org/10.1186/1756-0500-5-367
31. Wang, J., Wang, W., Kollman, P.A., and Case, D.A., *J. Mol. Graph. Model.,* 2006, vol. 25, p. 247. https://doi.org/10.1016/j.jmgm.2005.12.005
32. Wang, J., Wolf, R.M., Caldwell, J.W., Kollman, P.A., and Case, D.A., *J. Comput. Chem.,* 2004, vol. 25, p. 1157. https://doi.org/10.1002/jcc.20035
33. Jorgensen, W.L., Chandrasekhar, J., Madura, J.D., Impey, R.W., and Klein, M.L., 1983, vol. 79. https://doi.org/10.1063/1.445869
34. Roe, D.R. and Cheatham, T.E., *J. Chem. Theory Comput.,* 2013, vol. 9, p. 3084. https://doi.org/10.1021/ct400341p